

The Design of Voltage and Current Acquisition Front-Ends for Brain-Machine Interface

Jie Yuan

Hong Kong University of Science & Technology
Clearwater Bay, Hong Kong SAR
Phone: +852-23588029, E-mail: eeyuan@ust.hk

Abstract

Non-invasive or minimally invasive brain-machine interface (BMI) is one of technology drivers leading to the future. The integration of the sensing electrode and the acquisition electronics is critical to reduce the invasiveness of a BMI device. A wide range of research has been actively pursued for the design of voltage and current acquisition front-ends. In this paper, the design fundamentals of both types of acquisition front-ends are discussed. The achieved state-of-art designs are compared.

1. Introduction

BMI is emerging as a technology with great future implication. Currently, BMI has a dilemma in signal acquisition. The spatial and temporal resolution of transcranial signal is too low for decoding. On the other hand, endocranial signal acquired on or below the cortex surface has good signal quality. Nonetheless, the invasiveness of such BMI devices detrimentally prevents them from wide adoption. Minimizing the invasiveness of BMI devices is critical to its future application.

A BMI device is expected to acquire physiological signals from neurons in various cortical regions. Voltage signal is the major signal of interest in existing BMI research. Nonetheless, neuro-transmitter release is a more direct signal with great significance to the bio-medical community [1].

Currently, a BMI sensing device is typically uses electrode array coupled to individual neurons or neuron groups. In a voltage sensing device, the capacitive coupled voltage signal is the signal of interest for the acquisition front-end. In a neuro-transmitter sensing device, the redox current from the electrode is the signal of interest for the acquisition front-end. Hence, two types of acquisition front-ends are needed for BMI.

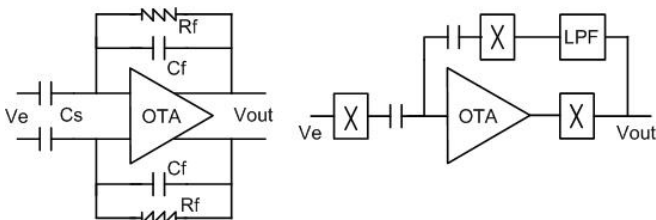


Fig. 1. bio-potential acquisition front-ends

2. Voltage Acquisition Front-end

The major challenge to acquire the bio-potential using the micro-electrode sensing device is the weak signal ($\sim 100\mu\text{V}$) on top of a slowly varying large electrode DC offset (up to V).

Hence, the acquisition circuits need to suppress the low-frequency offset while amplify the high-frequency signal with a very high gain ($>60\text{dB}$). Bio-potential from a single cell can have bandwidth up to 10kHz, while it is much narrower to record from a group cell. Over the years, two architecture has been developed to acquire bio-potentials as shown in Fig. 1.

Capacitive amplifier with a large feedback resistor is a commonly used voltage front-end due to its simplicity [2]. The zero formed by R_f and C_f determines the cut-off frequency of the low-frequency high-pass corner. The capacitor ratio C_s/C_f forms the mid-band gain. As C_f is normally small (fF) to enable large gain, R_s needs to be really high to enable a low cut-off corner ($<1\text{Hz}$). The main problem of this front-end is the OTA flicker noise dominates in the low frequency end. This flicker noise can be reduced by enlarging the transistors in the OTA, which unfavorably increases the noise gain of the amplifier due to the increased OTA gate capacitance. An optimization procedure was developed in [5] to achieve the lowest flicker noise for any given circuit area.

To acquire low-frequency bio-potential signals, such as ECG signal, feedback amplifiers with chopping have been designed to up-convert the signal to the thermal noise zone to avoid the flicker noise contamination [3]. The DC offset is filtered out and suppressed through the feedback, while the signal pass through the amplifier directly. Nonetheless, chopping increases the power consumption.

For power-sensitive implantable BMI devices with large array of acquisition channels, power efficiency is critical. For voltage amplifiers, a power noise efficiency factor (NEF) was defined in [2] as a ratio between the current of a voltage amplifier (I_D) and the theoretically needed minimum current to achieve its noise (v_{ni}).

$$NEF = v_{ni} \sqrt{\frac{2\beta I_D}{\pi \cdot 4kT \cdot U_T \cdot BW}} \quad (1)$$

3. Current Acquisition Front-end

The major challenge to acquire the redox current signal from a micro-electrode sensing device is the weak current signal ($\sim \text{pA}$) and a heavy capacitive electrode. The heavy capacitive load demands a very low impedance from the acquisition circuits to suppress voltage variation on the electrode [6]. Otherwise, the weak current signal can be buried by the electrode-induced current. This requires feedback to interface the electrode. Another challenge for current front-end is to handle the wide signal range, which could last over 5 decades.

There are different ways of quantizing the wide current

range in the back end. However, the front-end has been mainly designed with two architecture as shown in Fig. 2.

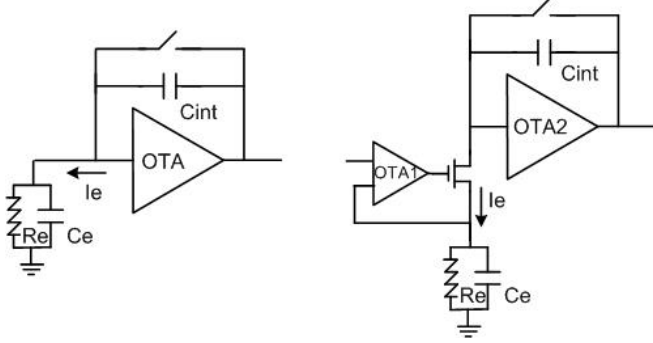


Fig. 2. The current acquisition front-ends

The current signal can be acquired by a capacitive TIA directly [4]. However, the electrode heavily loads the OTA input, which demands very wide OTA bandwidth. This needs very high power from the OTA to settle the electrode.

To improve the power efficiency, current buffers were used in the front-end to decouple the electrode load from the OTA [5]. In this design, the current buffer can be optimized to settle the electrode, while the TIA can be optimized to amplify the current.

4. Design Comparison

Table I shows a comparison of benchmark voltage front-end designs. It is clear that capacitive amplifier can achieve wide bandwidth. Over the wide bandwidth, capacitive amplifier can achieve NEF around 3 reliably.

Table I. Benchmark voltage front-end designs

	2003JSSC	2009JSSC	2010JSSC	2013ISSC	2013VLSI	2015TBCAS	2007TBCAS	2012JSSC	2012JSSC	2009JSSC	2016TBCAS
Sensory Mechanism	Electrical	Electrical	Electrical	Electrical	Electrical	Electrical Stim.	Electrical	Electrical	Electrical	Electrical Chemical	Elec. / Chem. Impedance
Channel	1	256	126	52	1024	256	1	96	2	4	100
Topology	CAFE	CAFE	CAFE	CAFE	CAFE	CAFE	CAFE	AC-amp	DC-amp	$\Sigma\Delta$	CAFE
Gain	40 dB	48-68 dB	0-80 dB	30-72 dB	Max78dB	53-72 dB	41 dB	40-56 dB	-	-	52-66 dB
$V_{in,max}$	16.7 μ V	4.4 μ V	-	18 μ V	-	-	7.3 μ V	-	3.5 μ V	\pm 25 μ V	5 μ V
BW	7.2 kHz	5 kHz	10 kHz	6 kHz	10 kHz	10-5 kHz	5.32 kHz	10 kHz	10 kHz	5 kHz	10 kHz
Noise [†]	2.2 μ V _{rms}	7 μ V _{rms}	2.4 μ V _{rms}	3.2 μ V _{rms} (300-6k)	2.4 μ V _{rms} (300-10k)	7.99 μ V _{rms}	3.06 μ V _{rms} (45-5.3k)	2.2 μ V _{rms}	4.9 μ V _{rms}	3.5 μ V _{rms}	4.07 μ V _{rms}
DR	78 dB	56 dB	-	75 dB	-	-	68 dB	-	57 dB	83 dB	62 dB
NEF	4.0 [‡]	4.6 [‡]	7.4	3.82 [‡]	3.7	8.99	2.67	4.5	6	11.1	3.51
Power	80 μ W	15 μ W	160 μ W	10.5 μ W	53.4 μ W	12.9 μ W	7.56 μ W	35 μ W	5.04 μ W	86 μ W	9.1 μ W
Technology	1.5 μ m	0.35 μ m	0.6 μ m	0.18 μ m	0.35 μ m	0.35 μ m	0.5 μ m	0.13 μ m	65 nm	0.5 μ m	0.18 μ m

Table II. Benchmark current front-end designs

	2008JSSC	2007TCAS1	2009TBCAS	2009JSSC	2006TCAS1	2009TBCAS	2013TBCAS	2016TBCAS
Sensory Mechanism	Chemical	Chemical	Electrical Chemical	Electrical Chemical	Chemical	Chemical	Chemical Impedance	Electrical, Chemical Impedance
Channel	16	42	1	4	16	1	96	100
Structure	TIA	$\Delta\Sigma$	$\Delta\Sigma$	$\Delta\Sigma$	CT buf 1-V	TIA	CT buf 1-F	DT/CT buf TIA
Range (I_{max})	\pm 110 nA	\pm 100n A	1p-1 μ A	\pm 750 nA	\pm 50n-50 μ A	\pm 20n A	350 nA	\pm 200p-50n A
BW _{sig,max}	1.25 kHz	125 Hz	<500 Hz	5 kHz	12 kHz	10 kHz	1 kS/s	110-10k Hz
Noise BW _{sig}	240 pA _{rms} (1.25 kHz)	30 pA _{rms} (100nA) 50 fA _{rms} (1pA)	200 pA _{rms} (\pm 400 nA, 125 Hz)	56.7 pA _{rms} (5 kHz) 7.4 pA _{rms} (50 Hz)	46 pA _{rms} (\pm 50 nA, 12 kHz)	5 pA _{rms} (10 kHz)	24 pA _{rms} (20 nA, 500 Hz)	93 pA _{rms} (50 nA, CT, 10 kHz) 30.5 pA _{rms} (50 nA, CT, 250 Hz) 21.6 pA _{rms} (50 nA, DT, 250 Hz) 0.48 pA _{rms} (200 pA, CT, 110 Hz)
Noise Density	6.79pA/Hz ^{0.5} (\pm 110 nA)	2.68pA/Hz ^{0.5} (100nA) 4.47fA/Hz ^{0.5} (1pA)	17.9pA/Hz ^{0.5} (\pm 400 nA)	0.80pA/Hz ^{0.5} 1.05pA/Hz ^{0.5} (\pm 750 nA)	0.42pA/Hz ^{0.5} (\pm 50 nA)	50 fA/Hz ^{0.5} (no bias)	1.07pA/Hz ^{0.5} (\pm 20 nA)	0.93pA/Hz ^{0.5} (50 nA, CT, 10 kHz) 1.93pA/Hz ^{0.5} (50 nA, CT, 250 Hz) 1.37pA/Hz ^{0.5} (50 nA, DT, 250 Hz) 46fA/Hz ^{0.5} (200 pA, CT, 110 Hz)
DR	59 dB	126 dB	120 dB	106 dB	127 dB	78dB	83 dB	104 dB
Power	625 μ W	11 μ W	42 μ W	76 μ W	780 μ W	300 μ W	188 μ W	12.1 μ W
Technology	0.25 μ m	0.5 μ m	0.5 μ m	0.5 μ m	1.2 μ m BiCMOS	SOI 0.5 μ m	0.35 μ m	0.18 μ m

Table II shows a comparison of benchmark current front-end designs. It is clear that TIA with current buffer can achieve lower noise than direct TIA front-ends, while direct TIA can achieve lower noise.

5. Conclusions

In this paper, design challenges of the voltage and current acquisition front-ends are discussed. Major voltage and current amplifier designs are illustrated and analyzed. The performance of state-of-art designs is compared.

Acknowledgements

The work described in this paper was supported by a grant from the RGC-NSFC joint scheme sponsored by the Research Grants Council of Hong Kong (Project No. N_HKUST615/14).

References

- [1] J. Guo, J. Yuan, J. Huang, J. K. Y. Law, C.K. Yeung, and M. Chan, IEEE J. Emerging & Selected Topics Circuits & Systems. 1 (2011) 461
- [2] R. Harisson and C. Charles, IEEE J. Solid-State Circuits. 38 (2003) 958.
- [3] R. Yazicioglu, P. Merken, R. Puers, and C. Van Hoo, IEEE J. Solid-State Circuits. 43 (2008) 3025.
- [4] P. Weerakoon, E. Culurciello, K. G. Klemic, and F. J. Sigworth, IEEE T. Bio. Circuits & Systems. 3 (2009) 117.
- [5] J. Guo and J. Yuan, IEEE T. Bio. Circuits & Systems. 10 (2016) 567.
- [6] J. Guo, J. Yuan, M. Chan, IEEE T. Bio. Circuits & Systems. 6 (2012) 605.